A low-cost PM$_{2.5}$ monitor for wildland fire smoke

Scott Kelleher[1], Casey Quinn[2] Daniel Miller-Lionberg[1], and John Volckens[1]

[1]Department of Mechanical Engineering, Colorado State University, Fort Collins, USA
[2]Department of Environmental and Radiological Health Sciences, Colorado State University, Fort Collins, USA

Correspondence to: John Volckens (john.volckens@colostate.edu)

Abstract.

Wildfires and prescribed fires produce emissions that degrade visibility and are harmful to human health. Smoke emissions
and exposure monitoring is critical for public and environmental health protection; however, ground-level measurements of

10 smoke from wildfires and prescribed fires has proven difficult, as existing (validated) monitoring technologies are expensive,
cumbersome, and generally require line power. Few ground-based measurements are made during fire events, which limits
our ability to assess the environmental and human health impacts of wildland fire smoke.

The objective of this work was to develop and validate an Outdoor Aerosol Sampler (OAS) - a filter-based air sampler that

15 has been miniaturized and weatherproofed. This sampler was designed to overcome several of the technical challenges of
wildland fire monitoring by being relatively inexpensive and solar powered. The sampler design objectives were achieved by
leveraging low-cost electronic components, open-source programming platforms, and in-house fabrication methods. A
direct-reading PM$_{2.5}$ sensor was selected and integrated with the OAS to provide time-resolved concentration data. Cellular
communications established via Short Message Service (SMS) technology were utilized in transmitting online sensor

20 readings and controlling the sampling device remotely. A Monte Carlo simulation aided in the selection of battery and solar
power necessary to independently power the OAS, while keeping cost and size to a minimum.

Thirteen OAS were deployed to monitor smoke concentrations downwind from a large prescribed fire. Aerosol mass
concentrations were interpolated across the monitoring network to depict smoke concentration gradients in the vicinity of the

25 fire. Strong concentration gradients were observed (spatially and temporally) and likely present due to a combination of
changing fire location and intensity, topographical features (e.g. mountain ridges), and diurnal weather patterns. Gravimetric
filter measurements made by the OAS (when corrected for filter collection efficiency) showed relatively good agreement with
measurements from an EPA federal equivalent monitor. However, the real-time optical sensor (Sharp GP2Y1023AU0F) within
the OAS suffered from temperature dependence, drift, and imprecision.

1. Introduction

30

Wildfires and prescribed fires are the largest combined source of primary fine particulate matter ($PM_{2.5}$) emissions into the atmosphere (NEI, 2014). These emissions degrade visibility and contribute to human morbidity and premature mortality (Sakamoto et al., 2016; Silva et al., 2013). Human exposure to biomass burning emissions has been associated with respiratory outcomes such as asthma, bronchitis, and COPD (Atkinson et al., 2014; Cohen et al., 2005; Gan et al., 2013) and cardiovascular

35 outcomes such as high blood pressure, stroke, and arrhythmia (Brook et al., 2004; Clark et al., 2013; Pope et al., 2004).

Fire regimes have changed during the last century due to changes in climate, land-management techniques, agricultural practices, and industrial development (Westerling et al., 2006). Over the past three decades, wildfires have increased in number, size, and severity (Alves et al., 2000; Miller et al., 2009). This upward trend of wildfire activity is predicted to persist in coming

40 years (Flannigan et al., 2000), meaning biomass burning will have an even greater impact on public and ecosystem health in the future (Spracklen et al., 2009; Yue et al., 2013). One method of wildfire mitigation is prescribed burning, a technique that has increased substantially in recent years.

The Interim Air Quality Policy on Wildland and Prescribed Fires was written by the EPA in 1998 to preserve public health

45 and wellbeing by mitigating air quality impacts from prescribed fires (EPA, 1998). Evaluating the effectiveness of smoke mitigation techniques is challenging, however, because emission and exposure monitoring data are sparse. Conventional instruments for monitoring wildfire smoke are expensive, costing $10,000 to $30,000 per unit (Strand et al., 2011). These instruments are large and typically require line power; thus, sampling locations are often limited to areas equipped with utility service and accessible by motor vehicle. Thus, few measurements are made during most fire events, which often results in an

50 incomplete representation of the fire's impact on local air quality (Hardy et al., 2001).

Satellite observations of air quality can be used to address ground-based monitoring gaps. Moderate resolution imaging spectroradiometer (MODIS) instrumentation, aboard the Terra and Aqua satellites, yield daily aerosol optical depth (AOD) measurements worldwide. AOD is an integrated extinction of light from the total mass of aerosol present in a vertical column

55 of the atmosphere; thus, AOD includes total aerosol mass at all elevations. Satellite-based aerosol measurements, however, still lack precision and fine spatial resolution and do not quantify air quality specifically at ground level (Lassman et al., 2017). As a result, a need still exists for spatially-resolved measurements of surface air quality in the vicinity of fires.

The objective of this work was to develop and validate a field-deployable, low-cost (under $500) $PM_{2.5}$ sampler that can run

60 autonomously with no external power. The sampler was intended to be remotely programmable and encapsulated in a lightweight, hardened enclosure. Specific design and performance objectives for the unit were: weigh less than 1000 grams (2.2 lbs), fit within a 3000 cm^3 (183 in^3) volume for ease of shipping, weatherproof, powered by solar and rechargeable battery,

capable of providing both online (via light scattering) and time integrated (via size-selective sampling onto a filter) measurements of $PM_{2.5}$, and capable of 1-2 week deployments. Following OAS development, a network of these low-cost

65 $PM_{2.5}$ monitors was deployed downwind from a prescribed fire to evaluate this device as a smoke-monitoring tool.

2. Methods

2.1 UPAS Technology

The Outdoor Aerosol Sampler (OAS) was based upon the Ultrasonic Personal Aerosol Sampler (UPAS) described previously (Volckens et al., 2017). The original UPAS was designed as a wearable device to estimate personal exposure to

70 $PM_{2.5}$ across a 24-hour period. A key feature of this sampler is a piezoelectric pump (which operates at ultrasonic frequency) that provides reductions in size, cost, and power relative to common diaphragm or rotary-vane air movers. The UPAS weighs 190 grams and has a bill-of-materials of approximately $300. The sampler contains a size-selective cyclone inlet for $PM_{2.5}$, a 37-mm air sampling filter, rechargeable batteries, a suite of environmental sensors (location by GPS, temperature, pressure, relative humidity, acceleration, light, and a real-time clock), and a miniature mass-flow sensor. Sample duration

75 and volumetric flow-rate through the instrument (1-2 L/min) can be programmed into the device using a smartphone application via Bluetooth connectivity (available on iOS and Android platforms). In prior laboratory tests, the UPAS performed well compared to both an EPA $PM_{2.5}$ federal reference method (URG cyclone model URG-2000-30EGN-A; URG Corp., Chapel Hill, NC, USA) and a personal $PM_{2.5}$ sampler (PEM 761-203; SKC, Inc., Eighty Four, PA, USA).

80 ### 2.2. OAS Development

The following additions and modifications were made to convert the UPAS from an indoor personal sampler into an outdoor area monitor: add a direct-reading $PM_{2.5}$ sensor, add cellular communications (Short Message Service, SMS), add battery capacity and solar charging, and harden the enclosure for all-weather operation. Additional modifications included developing a cartridge-style filter-holder (to simplify filter exchange in the field and to minimize sample contamination),

85 replacing the press-fit inlet cap with a threaded aluminum inlet, and modifying the housing to allow the device to be mounted into a weatherproof case.

Remote communications were accomplished by adding Short Message Service (SMS) technology, which allowed the OAS to be controlled via cell phone (or any device with internet access) and to report data back to a server. The built-in SMS

90 technology and predesignated communication protocol of a Particle Electron (Particle Industries Inc., San Francisco, CA) was utilized for this purpose. The Electron also features a microcontroller that was integrated into the UPAS circuitry, enabling communication among all components.

The online PM$_{2.5}$ sensor selected for this work was the Sharp GP2Y1023AU0F, which has been evaluated previously (Wang

95   et al., 2015). This light-scattering detector was envisioned to serve as a trigger mechanism, in addition to providing

continuous measurements of PM concentration. The sensor could prompt the OAS to begin sampling gravimetrically once a

threshold of aerosol concentration was exceeded. The prompt from the real-time sensor could also serve as an early warning

alarm (transmitted via on-board SMS technology) for an approaching smoke plume. Thus, the majority of OAS systems

could remain idle until a smoke plume is detected, which would help to conserve battery life.

100

A Pelican 1020 Micro Case was modified to enclose the OAS and to protect the unit from adverse weather. The mass-flow

sensor within the unit (Omron model DP6F) is dependent on air density, which can vary as a function of temperature,

humidity, and pressure. These variables were monitored in real-time and used to correct mass-flow readings (Volckens et al.,

2017). The UPAS creates a small amount of heat during operation as a by-product of battery discharge and pump work.

105   Therefore, pump exhaust was routed through the case (and out a series of small exit holes on the underside) to help maintain

a temperature inside the case near ambient. At 2 L/min of flow, approximately four air exchanges take place within the case

each minute. Shielding provided by the solar cells reduces OAS internal heating due to the absorption of solar radiation.

The OAS's two configurations are shown in Fig. 1.
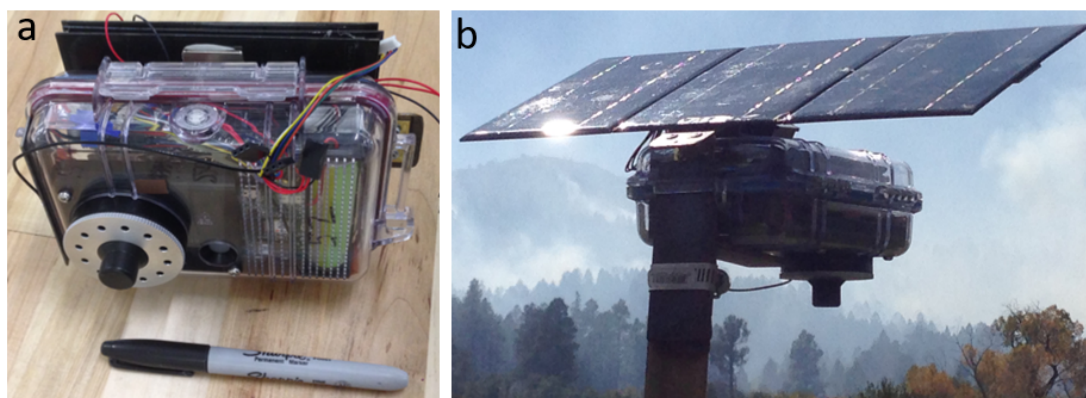
110

Figure 1. OAS sampler in (a) transportation configuration and (b) deployment configuration.

Table S1 lists the components added to the UPAS in the development of the OAS. The block diagram in Fig. 2 depicts the

basic components of the UPAS (colored grey) and the additional components added to create the OAS (colored blue).
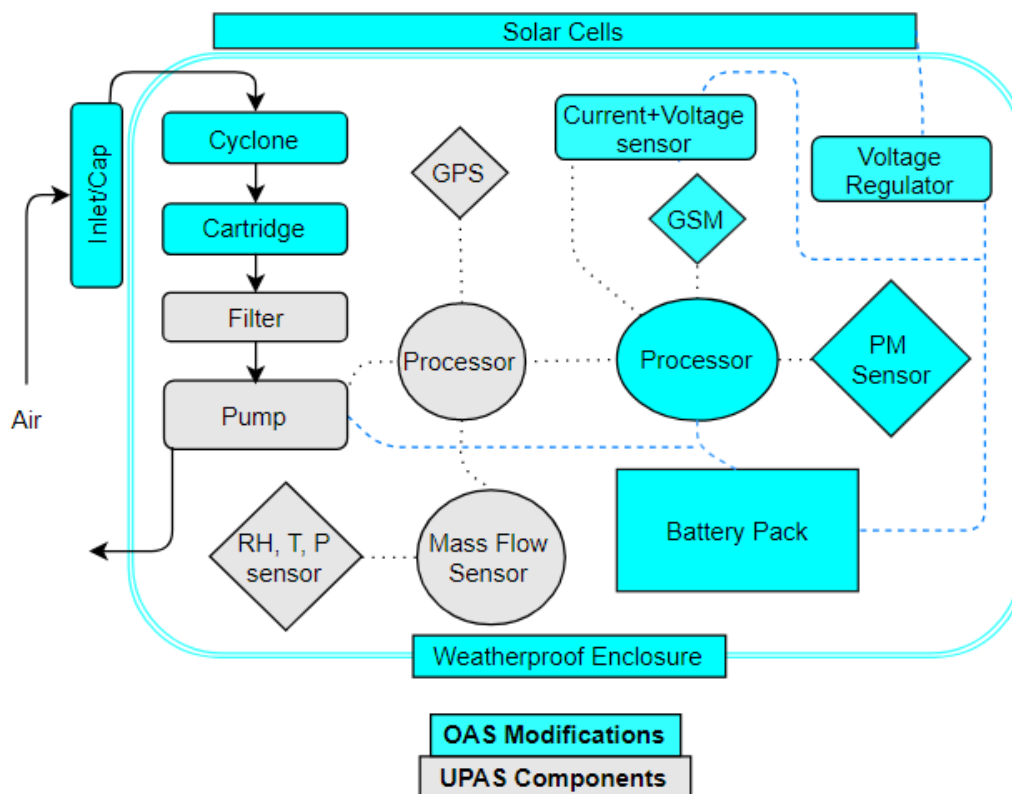
Figure 2. Block diagram of UPAS technology with component integration to form the OAS: GSM (Global System for Mobile Communications), PM (particulate matter), GPS (Global Positioning System)

2.3 Power System Design

120   Monte Carlo simulations were conducted to inform the selection of OAS solar and battery power. These simulations were designed to predict the probability of OAS power failure as a function of sampling duration (days), time of year (month), available solar irradiance, solar cell size, and battery capacity. Solar irradiance, the Monte Carlo sampled input variable, is defined as the daily average of observed solar irradiance attuned for solar cell size (0.014m^2 each). Solar irradiance data were obtained from the Christman Field weather station in Fort Collins, CO (CSU, 2016).

125

The simulation accounted for the following operational parameters: useable battery capacity, stationary solar conversion efficiency, temperature effects on battery capacity, charging circuit efficiency, and average OAS power consumption at 2 L/min of sample flow. Power consumption also varies depending on filter type and filter loading, but for these simulations a power consumption rate of 0.7 Watts was assumed (the approximate OAS power draw at 2 L/min of flow through a 37mm

130 Pallflex T60A20 Fiberfilm filter). One thousand iterations of 14-day sampling periods, for each month of the year, were simulated to calculate runtime (in days) for each iteration. The probability of power failure (for a series of consecutive sampling days across a particular month) is equal to the total number of failures specific to that day divided by the number of iterations simulated. This calculation was repeated to estimate a failure probability for each of the 14 consecutive days that were simulated across each month of the year. Monte Carlo simulations were run for varying numbers of solar panels (1-3

135 panels) and battery cells (2-5 cells).

The solar cell arrangement was designed to be collapsible to maintain a slender profile for easy transportation and shipping. A magnetically coupled bracket that is adjustable for optimum zenith-angle holds the solar cells rigidly in place while in deployment and transportation configuration (Fig. 1). A voltage regulator was added to the OAS battery charge controller to

140 condition electricity from the solar cells to 5 volts DC.

2.4 Prescribed Fire Sampling

Thirteen OAS units were arrayed in the vicinity of a 6000-acre prescribed fire (known as the Pargin Mountain fire), with assistance from the Colorado Department of Public Health and Environment (CDPHE) and the US Forest Service (USFS).

145 The fire took place 14 km east of Bayfield Colorado from September 8th through September 17th 2016. The OAS network was deployed prior to fire ignition, typically downwind and downslope from expected fire regions, following input from USFS overseers. Other considerations for sampler placement included: cooperation from land owners, non-obtrusive to fire operations, potential for livestock interference, and ease of access. Each OAS was placed a minimum of 60 m from the nearest roads to avoid the influence of road dust emissions.

150

A map of sampler locations and the area burned is shown in Fig. 3. The USFS monitored air quality during the prescribed burn by placing instruments at location 9 (E-SAMPLER, Met One Instruments, Grants Pass, OR) and location 1 (E-BAM, Met One Instruments, Grants Pass, OR). Two OAS were co-located with each USFS monitor at these locations. For the duration of the fire, each OAS was programmed to sample $PM_{2.5}$ for 24 hours onto 37mm Tisch PTFE filters (model SF17382) at a flowrate

155 of 2 L/min. The experimental design originally called for the use of Pallflex Fiberfilm T60A20 filters but these were discontinued by the manufacturer; Tisch PTFE filters were selected as an alternate. Flow through the OAS was checked pre- and post-sampling using a soap-bubble calibrator (A.P. Buck, Inc. Orlando, FL, USA).

Solar energy conversion efficiency was evaluated for each OAS and across all sampling periods. Data from the voltage/current

160   sensor on the OAS circuit board were used to determine the ratio of solar energy delivered to OAS batteries relative to available

solar irradiance. Hourly irradiance measurements were provided by a weather station (PRAWS 5) located on Pargin Mountain

during the month of September 2016.
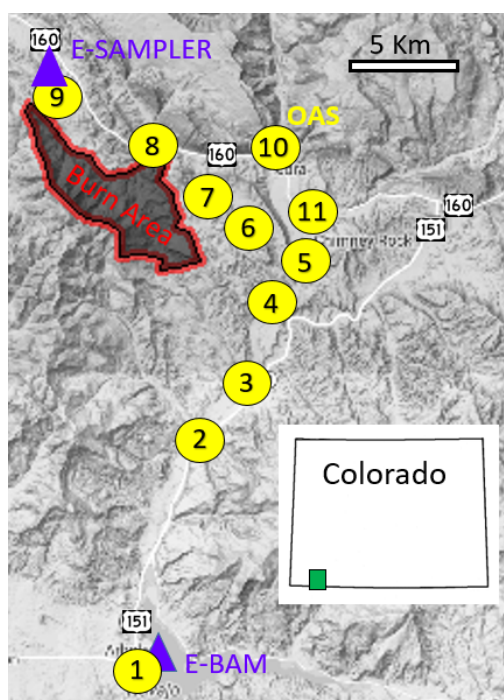
165   **Figure 3.** Location of monitoring equipment with respect to prescribed fire. OAS (yellow circles), US Forest Service equipment (blue
triangles), prescribed fire (shaded black area with red outline). Map elements created using ggplot (Kahle and Wickham, 2013).

2.5 Sample and Data Analyses

Filters were contained in individual filter-keepers, inside sealed plastic bags, for both transportation and storage. Filters were

170   placed in an equilibrium chamber for at least 12 hours before pre- and post-weighing and discharged on a polonium-210 strip

for a minimum of 15 seconds prior to weighing on an analytic microbalance (Mettler Toledo XS3DU; ± 1 µg). Three readings

were averaged together to determine each filter weight and field blanks were carried for all deployment days. Following post-

weigh analysis, the filters were placed in filter keepers (SKC 225-8303) and sealed in air tight bags and stored at -20 °C.

175 Descriptive statistics were calculated for all mass concentration data, including identification of outliers, which were primarily cases when the OAS was explicitly known to have malfunctioned (stopped sampling, underflowed, etc). For OAS performance comparison with respect to USFS equipment, measurements were considered valid if the sampler spanned more than 75 percent runtime and flow remained within 20 percent of desired control. Limit of detection for gravimetric measurements was defined as the average blank mass gain plus three times the standard deviation of the change in blank mass. Limit of quantification

180 was defined similarly but using five times the standard deviation in blank mass change.

Data analyses were conducted using Excel 2016 (Microsoft Corp., Redmond, WA, USA), Matlab 2015 (The MathWorks Inc., Natick, MA) and R 3.3.2 (R Core Team, Vienna, Austria). Spatial interpolation prescribed fire sampling results was based on ordinary kriging methods and plotted using gstat in R (Benedikt et al., 2016; Pebesma, 2004). Model interpolations were

185 constrained to an area (search radius) no more than 3km from a given sampler location. Performance evaluation of the OAS relative to E-BAM utilized an errors-in-variables model (Deming regression) to estimate a linear fit between methods.

3. Results and Discussion

Several key modifications helped streamline the use of the OAS in the field. The replaceable filter cartridge (Figure S5b) eliminated the need for direct filter handling in the field (during change outs), which reduced the risk of contamination and

190 also aided in sample transport. A threaded aluminum inlet cap (Fig. S5) sealed the filter cartridge in place and provided a rough inlet to protect against intrusion by small insects. The added costs (bill of materials) to convert the UPAS into the OAS totalled $183 for a single unit (Table S1).

3.1 Power

195 Power failure probabilities (representing the chance the OAS will experience power failure before the conclusion of a given number of consecutive sampling days) are shown Fig. 4 for the month of April. These results demonstrate the trade-off between run duration and the quantity of solar panels and battery cells inside the OAS (Fig. 4). Based on these simulations, a final design consisting of three solar panels ($0.042m^2$ total) and five battery cells (totalling 54 watt-hours of capacity) was chosen. This configuration maximized OAS run duration while also meeting specified design criteria for instrument cost,

200 size, and weight.
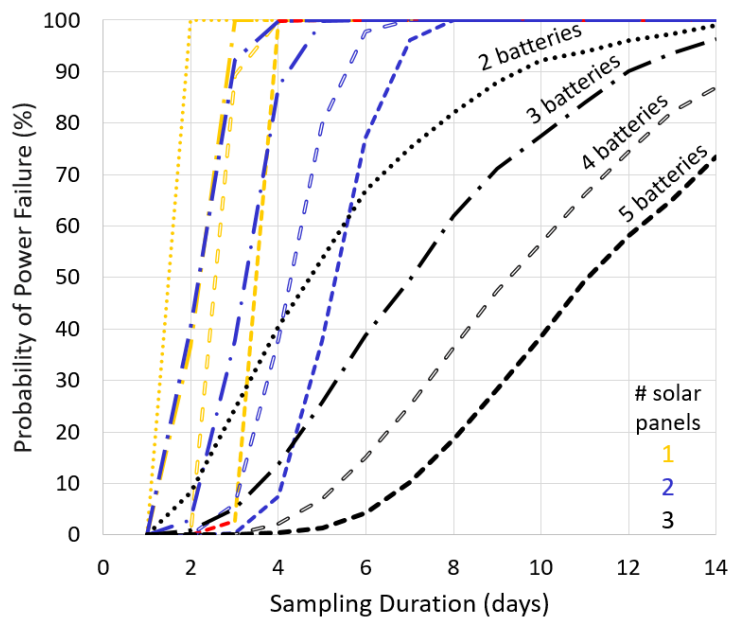
Figure 4. Probability of OAS power failure evaluated for various power designs (number of solar and battery cells) as a function of the number of continuous sampling days. Colors represent the number of solar panels (0.014m^2 each) and line type represents number of Li-ion
205   batteries (10.78 W-hrs. each) included.

Power failure probabilities for the final OAS design are shown in Fig. S1 for six months of the year. The simulation results suggest that the OAS can achieve three full days of continuous sampling during late fall and winter, greater than four days in Spring months, and a full week of continuous sampling in Summer. The internal battery, when fully charged, allows for two
210   full days of continuous sampling for all months of the year, regardless of the availability of solar power.

The Monte Carlo simulation was based on data from Fort Collins, Colorado between 2011 and 2015. Weather patterns, a large driver of solar irradiance available, are expected to vary by region. Thus, these simulation results are not generalizable beyond the Colorado Front Range. Further, the simulation selected random days within the specified month (i.e., blocks of
215   consecutive days were not sampled) for any of the 4 years. Random selection of days can attenuate the effect of large weather systems, which may also impact OAS runtime.

3.2 Prescribed Fire

An early morning photo (Fig. 5) taken September 18, 2016 from Chimney Rock National Monument facing west shows the

220   location of samplers in the OAS network during the Pargin burn. Smoke from the smouldering fire (red arrows) is observed

down slope in the valley bottoms. An image captured on the morning of Sept 17th from a relay station (Fig. 6), 2.4 kilometres

northwest of location 9 facing east, depicts the OAS network from a second view point.
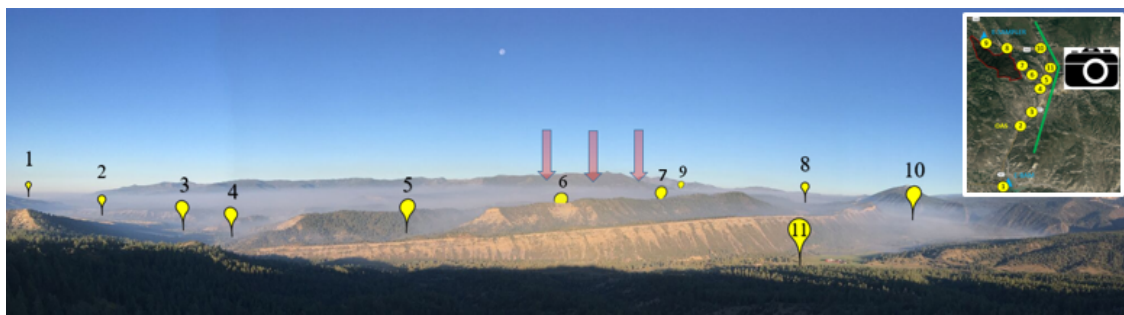
225   **Figure 5.** View from Chimney Rock, facing west on the morning of Sept. 18, 2016 when smoke is visible in several valleys. (Photo courtesy of Columbine Wildfire Management). OAS locations depicted by yellow markers. Visible smoke is observed around several OAS while other locations appear to be smoke free. Red arrows indicate location of prescribed fire operations.

230   **Figure 6.** Smoke covering valley floors caused by an inversion on the morning of Sept 17th, 2016. Photo taken from relay station 2.4 km northwest of Vance Ranch (location 9) facing east. (Photo courtesy of Columbine Wildfire Management)

The well characterized Pallflex Fiberfilm line of filters (originally intended for use within the OAS) was discontinued during

this project; an alternative filter (Tisch PTFE) was selected. Tisch PTFE filters were selected because they exhibit a relatively

235   low pressure drop and are comprised of hydrophobic polytetrafluoroethylene, which is less susceptible to organic vapor

adsorption artifacts than other fibrous filter materials (Kirchstetter et al., 2001; Mader and Pankow, 2001). Prescribed fire

sampling results suggested a non-ideal collection efficiency for accumulation-mode aerosol using the Tisch PTFE filters. Subsequent laboratory tests, using a previously described protocol (Cardello et al., 2002), confirmed the relatively low collection efficiency of these filters (results shown in Fig. S2). The estimated mass collection efficiency of these filters was

240   66.7%, assuming a size distribution for an unaged biomass burning aerosol (Sakamoto et al., 2016). Mass concentration data reported here have been corrected for filter collection efficiency.

A total of 61 OAS deployments were made over the nine-day prescribed fire. Seventeen of the sixty-one deployments failed to complete an intended measurement. Approximately half of these failures (Fig. S6) were due to battery premature power

245   failure, which, in turn was the result of filter overloading from extremely high PM concentrations. Analysis of filter pressure drop data (collected on board each OAS) and filter mass accumulation revealed that these devices ran out of battery power as a result of high mass loadings on filters. Results from those samplers (typically where 24-hr $PM_{2.5}$ concentrations exceeded 200 µg/m^3) have been extrapolated out to a 24-hr average; thus, they represent a lower bound of average mass concentration for that site and sampling day. Samplers that ran for less than 18 hrs (n=17), regardless of measured concentration, were not

250   included in the final analyses.

Data mapping and interpolation techniques (ordinary kriging) were used to investigate the spatial and temporal evolution of ground-level $PM_{2.5}$ concentrations from September 12th through September 18th, 2016. Maps illustrating interpolated mass concentrations for September 10th, 12th, and 18th are shown in Fig. 7. Results from September 15th, and 17th are shown in Fig.

255   S3. Aerosol mass concentrations are colored to depict concentration gradients for the following ranges: green, concentrations at or below the National Ambient Air Quality Standards (NAAQS) annual $PM_{2.5}$ limit (12µg/m^3); yellow, concentrations falling between the annual limit (12µg/m^3) and the NAAQS 24-hour $PM_{2.5}$ limit (35µg/m^3); orange, concentrations falling between the 24-hour NAAQS limit (35µg/m^3) and 100µg/m^3; and red, concentrations in excess of 100 µg/m^3. Average, 24-hr mass concentrations are labelled at each individual sampling site on each map. Wind speed and direction data during each 24-

260   hour sampling period are illustrated by a wind rose located to the right of each map. These interpolated concentration maps depict aerosol concentrations near the fire ranging from less than 15µg/m^3 to over 500µg/m^3 across the sampling campaign.
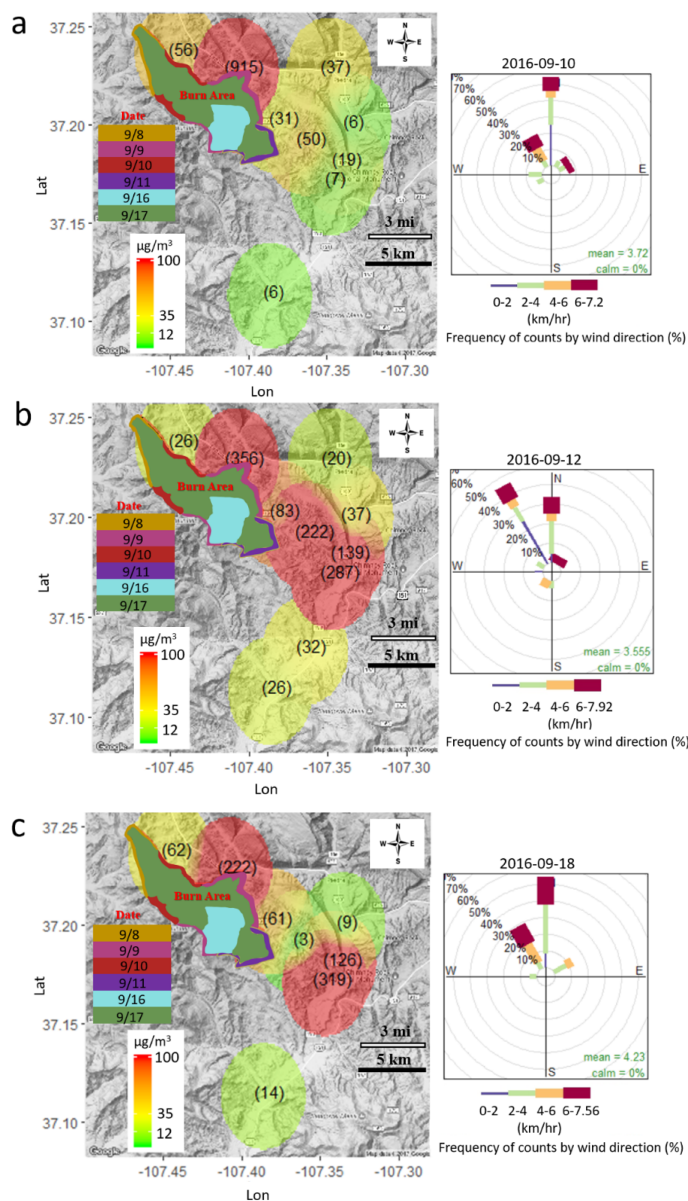
Figure 7. Maps illustrating spatial concentration gradients and the temporal evolution of fire emissions for (a) Sept 10th, (b) Sept 12th, and (c) Sept 18th of 2016. Numbers indicate 24-hour average mass concentration at each sampling site (e.g. '57' refers to a mass concentration of 57 µg/m^{3}). Dates represents the location and area burned each day with respect to the total prescribed fire.

A time series depicting variability of daily PM$_{2.5}$ concentrations measured across the OAS network is shown in Fig. 8.
Measurements made by the US Forest Service air quality monitoring equipment (E-SAMPLER and E-BAM) are also shown
as red and turquoise lines, respectively. The OAS network captured a wide range of PM$_{2.5}$ concentrations; this range was
captured by the two USFS monitors on only two of the five deployment days. Thus, the OAS network provided a more
spatially comprehensive assessment of smoke impact in the immediate vicinity of the prescribed burn. One key advantage of
the OAS, in this regard, is that monitoring can take place in remote areas that lack line power (necessary to operate
equipment like the E-BAM and E-SAMPLER). On several days the OAS network reported nearly 100-fold changes in 24-hr
average PM$_{2.5}$ concentrations between sites that were separated by only a few kilometres, further demonstrating the high
spatial variability in smoke plume concentrations emitted by the fire.

The real time optical sensor (Sharp GP2Y1023AU0F) integrated with the OAS was determined to be unreliable for
measuring PM in an outdoor setting. The sensor was affected by meteorological variables and inconsistent drift patterns,
which precluded the use of this sensor as a trigger for the gravimetric sampler. The Sharp sensor's output voltage with
respect to ambient temperature is displayed in Fig. S4, demonstrating a strong linear trend. A second issue with the Sharp
sensor was baseline drift, which spanned as much as 50 μg/m^3 on some days. Unfortunately, the baseline drift was neither
predictable nor correctable during the outdoor deployment (anecdotally, this drift was much less apparent during laboratory
testing in a controlled environment). Collectively, these issues precluded the ability to establish a baseline concentration
(without in-situ calibration) prior to each deployment, even with a co-located gravimetric reference sample. Further work on
the practicality of the Sharp sensor for remote outdoor sampling is warranted.
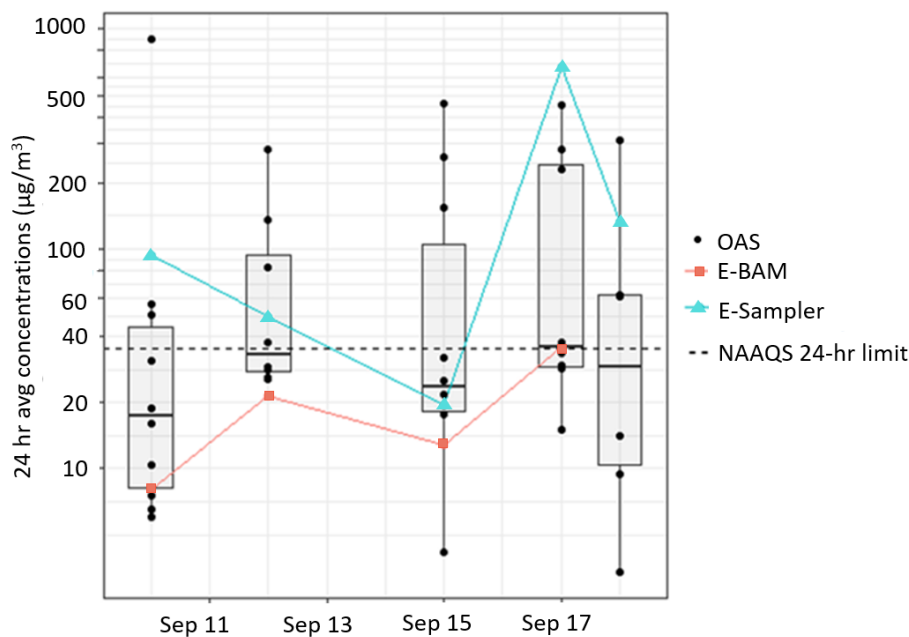
Figure 8. Prescribed fire summary of air quality at all locations for all dates sampled by both OAS and Forest Service equipment (E-BAM
290   and E-SAMPLER). OAS concentrations displayed fit the following criteria: sample more than 75% of 24-hour sampling period and
remain within 20% of desired flow control at all times.

A performance comparison between the OAS and E-BAM (co-located at Arboles Fire Station, location 1) is shown in Fig. 9.
The E-BAM measures PM mass concentrations using Beta attenuation and has been shown to agree closely with FRM

295   monitors (Trent, 2006). A Deming regression of the E-BAM and OAS yields a slope of 1.01 and an intercept of -5.9 µg/m^3.
The intercept may be due to error in the estimated mass collection efficiency of the Tisch PTFE filters for biomass burning
aerosol. However, the agreement between the two instruments is still relatively good (R^2 = 0.92), despite the small sample
size (n =7).

300   Solar power harvested by the OAS was compared to solar irradiance data for the duration of the prescribed burn sampling.
On average, 6.7% of incident solar energy was converted into useful battery power by the OAS. Solar conversion efficiency
measured in the field was slightly less than the 7.5% efficiency input to the Monte Carlo simulation. On average, however,
the solar circuit added an average of 11 hours runtime to the OAS during a given 24-hour period.

E-BAM (µg/m³) = -5.88 + 1.01·OAS
R^2= 0.92
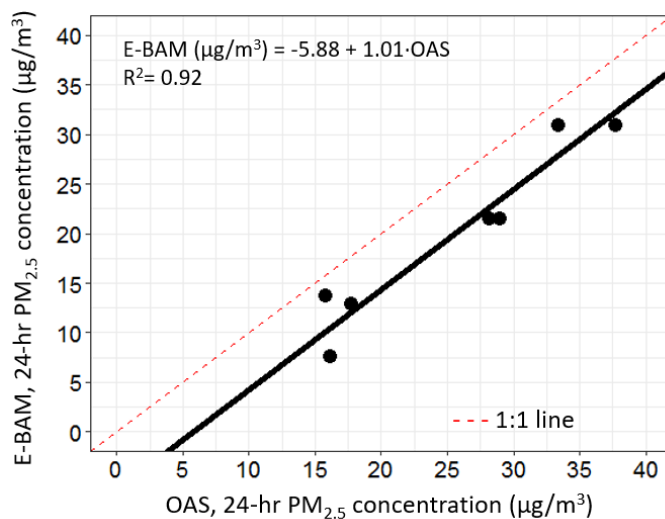
305

Figure 9. Performance of the Outdoor Aerosol Sampler relative to an E-BAM federal equivalent Monitor (meets US-EPA requirements for Class III designation for $PM_{2.5}$) at location 1.

3.3 Limitations and Future Work

310 The thirteen OAS samplers deployed in a network on the prescribed fire captured high concentration gradients resulting from smoke. Actual gradients, however, may have been even stronger than what was measured. One method of improving the spatial resolution of the network would be to deploy more OAS units. However, given the terrain features for the Pargin burn, only about 15 OAS units could be feasibly deployed by a single person in a 24-hr period.

315 The assumption of a fixed OAS power consumption did not allow the simulation to account for high filter loadings and the associated increased OAS power consumption. High aerosol concentrations (i.e., > 200 µg/m³) also reduced the OAS runtime due to excessive filter loading rate. Future work should consider strategies to improve runtime when sampling extremely high aerosol concentrations, such as the use of intermittent sampling flow via duty cycle.

320 A hindrance of the remote communications method used is the limited availability of the Particle hosted service. The service is only available while the Particle Electron is online, resulting in increased power consumption if communication is to be maintained at all times. Another issue is the execution frequency permitted by Google Scripts. Google Scripts is a free service; however, execution frequency limits data collection to once per hour. A possible solution addressing the limited availability

of the Particle web page would be the use of an interrupt queue. This prompt would significantly reduce server time and power

325 consumption. A personal server designed for OAS communication would alleviate issues associated with data collection frequency and simplify data archiving.

The Sharp sensor suffered from unpredictable drift issues, rendering the real-time measurements unreliable. Although post-sampling calibration (i.e., normalizing the sensor data to the 24-hr filter mass concentration) would alleviate some of this error,

330 the baseline drift issue would still produce a substantial bias in reported PM concentrations. Possible OAS improvements include replacing the real-time sensor (Sharp) with a more reliable PM sensor. Low cost $PM_{2.5}$ optical sensing technology is an active area of research and development; future iterations of the OAS technology should seek to improve this capability. An accurate, reliable low-cost sensor would enable the OAS to monitor air quality while remaining in an idle state. Utilizing the low-cost sensor as a trigger mechanism (as originally intended) would allow an OAS network to serve as an early warning

335 tool by detecting and tracking emissions in real time.

4. Conclusions

Reference instruments used to assess outdoor air quality tend to be expensive and bulky. This project developed and tested an Outdoor Aerosol Sampler (OAS) that is compact, weatherproof, battery powered, and designed to approach reference-quality

340 measurements of $PM_{2.5}$. The OAS achieved a relatively compact size (17 x 12 x 10 cm), a low weight (888 grams) and quiet operation. The inclusion of solar and additional battery power allowed the OAS to be successfully deployed for several days at a time. The integration of wireless remote communications provides control of the OAS from distant locations and data transmission in real-time. A durable weatherproof enclosure and solid mounting system allowed the OAS to be operated during all months of the year, through strong winds, rain, and snow.

345

Thirteen OAS were deployed around a large prescribed fire in southern Colorado to evaluate its effectiveness as a smoke monitoring tool. The OAS network provided spatially resolved measurements in regions where sampling with current state-of-the-art equipment was not possible. Strong concentration gradients were observed and likely present due to topographical features (e.g. mountain ridges) and diurnal weather patterns. At extremely high concentrations (i.e., 24-hr $PM_{2.5}$ > 200

350 $\mu g/m^3$), the OAS units were prone to power failure due to overloading of the sampling filter.

The cost, independent power capability, and compactness of the OAS provide a practical means for more effective monitoring of smoke from a prescribed burn or wildfire event. A successful demonstration of a low-cost sensor network represents a first step towards providing burn managers, state and federal agencies, and concerned citizens with a better understanding of fire

355 smoke emissions and resulting exposures. The OAS is not limited to fire events only and may be used for many other

applications of outdoor air quality monitoring. At nearly 1/20th the cost of current state-of-the-art field monitoring equipment, the OAS may be deployed in higher quantities under the assumption of fixed fiscal resources. Air quality data at more locations has the potential to enhance the accuracy of exposure models, yielding a more comprehensive estimate of potential human and environmental health hazards from smoke.

360

5. Data availability

A .csv file of 24 hour concentrations, start stop times, locations

Acknowledgements

The authors wish to thank the following individuals for their contributions to this work: Josh Smith for software and firmware
365 development; Nick Good, John Mehaffy, Christian L'Orange for assistance with field sampling and data analysis methods; John (Jay) Godson (USFS), Sarah Gallup (CDPHE), Pat McGraw (CDPHE), and Ken Helcoski (CDPHE) for their coordination with field sampling. This research was funded by a cooperative agreement from the Joint Fire Science Program (16-2-01-3).

References

370 Alves, C. A., Pio, C. A., and Duarte, A. C.: Particulate Size Distributed Organic Compounds in a Forest Atmosphere, Environmental Science and Technology, 34, 4287-4293, 2000.

Atkinson, R., Carey, I. M., Kent, A. J., Van Staa, T., Anderson, H., and Cook, D. G.: Long-term exposure to outdoor air pollution and the incidence of chronic obstructive pulmonary disease in a national English cohort, Occupational and environmental medicine, 2014. oemed-2014-102266, 2014.

375 Benedikt, G., Pebesma, E. J., and Heuvelink, G.: Spatio-Temporal Interpolation using gstat., R Journal, 8, 204-218, 2016.

Brook, R. D., Franklin, B., Cascio, W., Hong, Y., Howard, G., Lipsett, M., Luepker, R., Mittleman, M., Samet, J., and Smith, S. C.: Air pollution and cardiovascular disease, Circulation, 109, 2655-2671, 2004.

Cardello, N., Vockens, J., Tolocka, M., Wiener, R., and Buckley, T.: Technical Note: Performance of Personal Electrostatic Precipitator Particle Sampler, Aerosol Science and Technology, 36, 162-165, 2002.

380 Clark, M. L., Bachand, A. M., Heiderscheidt, J. M., Yoder, S. A., Luna, B., Volckens, J., Koehler, K. A., Conway, S., Reynolds, S. J., and Peel, J. L.: Impact of a cleaner-burning cookstove intervention on blood pressure in Nicaraguan women, Indoor Air, 23, 105-114, 2013.

Cohen, A. J., Ross Anderson, H., Ostro, B., Pandey, K. D., Krzyzanowski, M., Künzli, N., Gutschmidt, K., Pope, A., Romieu, I., and Samet, J. M.: The global burden of disease due to outdoor air pollution, Journal of Toxicology and Environmental Health, Part A, 68, 1301-1307, 2005.

385

CSU: Christman Field Weather Station. 2016.

EPA: Interim Air Quality Policy on Wildland and Prescribed Burns. Agency, E. P. (Ed.), RTP, NC, 1998.

Flannigan, M. D., Stocks, B. J., and Wotton, B.: Climate change and forest fires, Science of the total environment, 262, 221-229, 2000.

390 Gan, W. Q., FitzGerald, J. M., Carlsten, C., Sadatsafavi, M., and Brauer, M.: Associations of ambient air pollution with chronic obstructive pulmonary disease hospitalization and mortality, American journal of respiratory and critical care medicine, 187, 721-727, 2013.

Hardy, C. C., Ottmar, R. D., Peterson, J. L., and Core, J. E.: Smoke management guide for prescribed and wildland fire: 2001 edition, 2001. 2001.

395 Kahle, D. and Wickham, H.: ggmap: Spatial Visualization with ggplot2, R Journal, 5, 144-161, 2013.

Kirchstetter, T. W., Corrigan, C. E., and Novakov, T.: Laboratory and field investigation of the adsorption of gaseous organic compounds onto quartz filters, Atmospheric Environment, 35, 1663-1671, 2001.

Lassman, W., Ford, B., Gan, R. W., Pfister, G., Magzamen, S., Fischer, E. V., and Pierce, J. R.: Spatial and Temporal Estimates of Population Exposure to Wildfire Smoke during the Washington State 2012 Wildfire Season Using Blended Model, Satellite,
400 and In-Situ Data, GeoHealth, 1, 106-121, 2017.

Mader, B. T. and Pankow, J. F.: Gas/solid partitioning of semivolatile organic compounds (SOCs) to air filters. 3. An analysis of gas adsorption artifacts in measurements of atmospheric SOCs and organic carbon (OC) when using Teflon membrane filters and quartz fiber filters, Environ. Sci. Technol., 35, 3422-3432, 2001.

Miller, J. D., Safford, H., Crimmins, M., and Thode, A.: Quantitative evidence for increasing forest fire severity in the Sierra
405 Nevada and southern Cascade Mountains, California and Nevada, USA, Ecosystems, 12, 16-32, 2009.

Pebesma, E. J.: Multivariable geostatistics in S: the gstat package. Computers & Geosciences, 30: 683-691., Computers & Geosciences, 30, 683-691, 2004.

Pope, C. A., Burnett, R. T., Thurston, G. D., Thun, M. J., Calle, E. E., Krewski, D., and Godleski, J. J.: Cardiovascular mortality and long-term exposure to particulate air pollution, Circulation, 109, 71-77, 2004.

410 Sakamoto, K. M., Laing, J. R., Stevens, R. G., Jaffe, D. A., and Pierce, J. R.: The evolution of biomass-burning aerosol size distributions due to coagulation: dependence on fire and meteorological details and parameterization, Atmospheric Chemistry and Physics, 16, 7709-7724, 2016.

Silva, R. A., West, J. J., Zhang, Y., Anenberg, S. C., Lamarque, J.-F., Shindell, D. T., Collins, W. J., Dalsoren, S., Faluvegi, G., and Folberth, G.: Global premature mortality due to anthropogenic outdoor air pollution and the contribution of past climate
415 change, Environmental Research Letters, 8, 034005, 2013.

Spracklen, D. V., Mickley, L. J., Logan, J. A., Hudman, R. C., Yevich, R., Flannigan, M. D., and Westerling, A. L.: Impacts of climate change from 2000 to 2050 on wildfire activity and carbonaceous aerosol concentrations in the western United States, Journal of Geophysical Research: Atmospheres, 114, 2009.

420   Strand, T., Larkin, N., Rorig, M., Krull, C., and Moore, M.: PM2.5 measurements in wildfire smoke plumes from fire seasons 2005–2008 in the Northwestern United States, Journal of Aerosol Science, 42, 143-155, 2011.

Trent, A.: Smoke Particulate Monitors: 2006 Update. USDA (Ed.), USFS, 2006.

Volckens, J., Quinn, C., Leith, D., Mehaffy, J., Henry, C. S., and Miller-Lionberg, D.: Development and Evaluation of an Ultrasonic Personal Aerosol Sampler (UPAS), Indoor Air, 27, 419-413, 2017.

Wang, Y., Li, J., Jing, H., Zhang, Q., Jiang, J., and Biswas, P.: Laboratory Evaluation and Calibration of Three Low-Cost
425   Particle Sensors for Particulate Matter Measurement, Aerosol Science and Technology, 49, 1063-1077, 2015.

Westerling, A. L., Hidalgo, H. G., Cayan, D. R., and Swetnam, T. W.: Warming and earlier spring increase western US forest wildfire activity, science, 313, 940-943, 2006.

Yue, X., Mickley, L. J., Logan, J. A., and Kaplan, J. O.: Ensemble projections of wildfire activity and carbonaceous aerosol concentrations over the western United States in the mid-21st century, Atmos. Environ., 77, 767-780, 2013.
430